

Plasticity of Porous NiTi Alloys Obtained by Self-propagating High-temperature Synthesis in Closed and Open Gas Flow Reactors

Ekaterina S. Marchenko, Yuri F. Yasenchuk, Oibek Mamazakirov, Anatoly A. Klopotov, Gulsharat A. Baigonakova, Alex A. Volinsky & Sergey V. Gunter

To cite this article: Ekaterina S. Marchenko, Yuri F. Yasenchuk, Oibek Mamazakirov, Anatoly A. Klopotov, Gulsharat A. Baigonakova, Alex A. Volinsky & Sergey V. Gunter (2023) Plasticity of Porous NiTi Alloys Obtained by Self-propagating High-temperature Synthesis in Closed and Open Gas Flow Reactors, *Materials and Manufacturing Processes*, 38:6, 659-667, DOI: [10.1080/10426914.2023.2165665](https://doi.org/10.1080/10426914.2023.2165665)

To link to this article: <https://doi.org/10.1080/10426914.2023.2165665>



Published online: 09 Jan 2023.



Submit your article to this journal [↗](#)



Article views: 45










View related articles [↗](#)



View Crossmark data [↗](#)



Plasticity of Porous NiTi Alloys Obtained by Self-propagating High-temperature Synthesis in Closed and Open Gas Flow Reactors

Ekaterina S. Marchenko ^a, Yuri F. Yasenchuk ^a, Oibek Mamazakirov ^a, Anatoly A. Klopotov ^a,
Gulsharat A. Baigonakova ^a, Alex A. Volinsky ^{a,b}, and Sergey V. Gunter ^a

^aLaboratory of Superelastic Biointerfaces, National Research Tomsk State University, Tomsk, Russia; ^bDepartment of Mechanical Engineering, University of South Florida, Tampa, FL, USA

ABSTRACT

Porous NiTi alloys were obtained by self-propagating high-temperature synthesis (SHS) using layer-by-layer combustion in closed and open gas flow reactors under a protective argon atmosphere. The maximum compressive strain of porous NiTi alloys synthesized in the closed reactor was 34% compared to 7% in the open gas flow reactor. X-ray diffraction, differential scanning calorimetry, scanning electron microscopy, energy dispersive spectroscopy, and optical microscopy showed that the reaction products in the two-phase gas zone of peritectic crystallization are in the form of isolated Ti₂Ni crystalline clusters in the TiNi matrix. The ductility and strength of the recrystallized Ti₂Ni phase hard dendrites increase the effective stiffness of porous NiTi alloys and decrease the maximum compressive strain. A highly porous NiTi alloy with improved mechanical properties was obtained by the SHS method in a closed reactor.

ARTICLE HISTORY

Received 22 August 2022
Accepted 7 December 2022

KEYWORDS

NiTi; biomaterials; implants; porosity; SHS; reactions; microstructure; recrystallization; properties

Introduction

NiTi porous alloys obtained by self-propagating high-temperature synthesis (SHS) have been used in clinical practice for more than 30 years as bone implant materials. They have found wide applications due to experimentally confirmed biochemical and biomechanical compatibility, high corrosion resistance, permeability, and manufacturability by the SHS method.^[1,2] Porous SHS-NiTi alloys differ significantly in terms of their structure and properties from alloys obtained by other methods, including powder metallurgy.^[1–5] Studies of the NiTi alloys' mechanical properties are important since the pore space of implants is filled with tissues and fluids, and is involved in the transfer of physiological load between bone fragments. Successful integration of an implant into the bone and soft tissues depends on the biomechanics of the porous implant-biological tissue-fluid composite.

It is known that NiTi SHS and reaction sintering^[6] happen with the obligatory participation of the melt.^[7] A porous frame made of the Ni+Ti powder mixture has some specific porosity and pore size distribution. It is impregnated and dissolved by the eutectic melt, forming new portions of the melt, which spread over the heated reaction layer of the powder mixture under the action of capillary forces. A heterogeneous chemical synthesis reaction of a new NiTi compound takes place on the surface of powder fragments in a liquid melt film. Eutectic and peritectic crystallization of the reaction products depends on the liquid concentration. The reaction propagates layer by layer, forming a reaction wavefront within the reaction boundaries. The reaction front propagation rate is controlled by the conductive heating of the charge, capillary spreading of the eutectic melt, and the transfer of the peritectic melt and heat

from the reaction gases. The formation of the reaction products is controlled by the heterogeneous solid–liquid reaction of the NiTi grains synthesis and the peritectic crystallization of the two-phase TiNi+Ti₂Ni surface zone. The phase composition of the porous alloy obtained by the layer-by-layer SHS in an open gas flow reactor was studied based on the previous work using the phenomenological approach. The effects of the powder mixture granulometric composition, bulk density, heating temperature and rate on porosity, pore size distribution, phase composition, formation of nonmetallic inclusions, degree of segregation in the peritectic crystallization zone, and concentration inhomogeneity of the TiNi phase in porous SHS-NiTi alloy were studied. The obtained results demonstrate common features of the porous SHS-NiTi alloy crystallization in all studied synthesis modes. At least two zones always form: the NiTi solid solution crystallization zone and the two-phase TiNi+Ti₂Ni peritectic crystallization zone.

The peritectic zone size depends on the thermal effects of the reaction gases. With a more intense thermal effect of the reaction gases in terms of temperature and time, large zones of peritectic crystallization are formed, and small zones are formed with less intensity but in larger quantities. The heat and mass transfer of the reaction gases is largely controlled by the thermal desorption of impurities and the dissolution of powders. The transfer of gaseous and solid impurities affects the geometry and specific surface area of the SHS-NiTi porous framework, the pore size distribution, and the interconnection of the reaction layers. The phase and concentration inhomogeneity of the synthesized porous NiTi alloys is the result of the above complex physicochemical factors.

The critical reversible martensitic transformation (MT) temperatures caused by thermal cycling under load are shifted due to changes in the TiNi phase concentration composition.^[8] Ni is nonuniformly distributed over the porous alloy since nonequilibrium crystallization and incomplete impurity segregation processes are characteristic SHS features.^[9]

Due to the inhomogeneity of the TiNi phase concentration in the alloy, there are sections that begin and end the martensitic transformation at significantly different temperatures simultaneously. Therefore, the critical temperatures of martensitic transitions are effective quantities. The elastic and plastic properties of porous NiTi can be modified by^[10–12]:

- (1) Homogenization annealing, which improves the synthesized alloy microstructure;
- (2) The SHS regime changes;
- (3) Precipitation hardening of the synthesized alloy by heat treatment.

Studying vacuum annealing effects on martensitic transformations in porous SHS-NiTi samples under load and temperature showed that annealing partially homogenizes the alloy phase composition, shifts the temperatures of martensitic transformations, and nonlinearly affects the maximum accumulated strain and the effective modulus of elasticity of porous samples.^[8]

Annealing in a vacuum was carried out at 300–1,000°C. The maximum increase in the total accumulated strain, the martensitic transformation temperature, and the decrease in the accumulated strain during phase transformation occur at 500–600°C. The detected anomalies of mechanical properties were attributed to nonlinear changes in the TiNi phase concentration composition and the volume fraction of the secondary Ti₂Ni phase with a monotonic annealing temperature increase.^[8] In reference,^[9] the authors studied the phase and elemental composition of porous SHS-NiTi alloys by scanning electron microscopy and energy dispersive spectroscopy after annealing in a vacuum at 300–1,000°C and found accumulations of the Ti₄Ni₂(O, N, C) phase inclusions and Ti₂Ni secondary phase crystals at the TiNi grain boundaries.

One of the ways to affect the SHS macro kinetics and alloy properties is to reduce the heat losses of the layer-by-layer combustion method by changing the direction of the reaction gases' movement in the reactor during synthesis from flow to circulation. However, little attention has been paid to this approach. The possibilities of homogenizing the phase composition and increasing the plasticity of porous NiTi alloys by the thermal action of reaction gases during SHS were studied in this work. The phase composition of porous samples synthesized in open gas/heat flow and closed reactors was compared to draw substantiated conclusions. The properties of samples obtained in an open reactor after additional annealing in a vacuum were also studied.

Materials and methods

Porous NiTi alloys were obtained from PTOM titanium powder and PNK-1L5 nickel powder in open gas flow and closed reactors using the SHS method. Schematics of the open gas

flow and closed SHS reactors are shown in Fig. 1. The powders were dried in a laboratory vacuum cabinet at 60–70°C for 6 hours and mixed in a V-shaped mixer for 8 hours. The powder mixture was poured into quartz tubes with a 40 mm inner diameter and compacted to 64–66% porosity, achieving uniform density and uniform distribution of powders throughout the volume of the workpiece. Then, the quartz tube with the charge was installed in the reactor and heated to 460–480°C in a laboratory tubular electric furnace in an Ar gas atmosphere for 20 min. The synthesis was initiated by a heated molybdenum coil at the open end of the powder preform. After completion of the synthesis reaction, the reactor with the resulting alloy was cooled in water without stopping the protective Ar gas flow.

The closed reactor was filled with inert gas and hermetically sealed before synthesis. The entire reactor was cooled to room temperature after synthesis using water cooling. Ten samples in the form of 6 × 3 × 3 mm³ prisms were cut by electrical discharge machining (EDM). Compression testing of porous samples was carried out using an INSTRON 3386 universal tensile testing machine at a compression rate of 0.005 sec⁻¹.

Scanning electron microscopy (SEM) of porous NiTi samples was performed using a Tescan Vega 3 microscope, and energy dispersive spectroscopy (EDS) elemental composition mapping was performed using an Oxford Instruments energy dispersive microanalysis system. X-ray diffraction phase analysis was performed using a Shimadzu XRD 6000 X-ray diffractometer with a Cu-Kα radiation at 40 kV and 20 mA. The PDF 4+ database with the POWDER CELL 2.4 full-profile analysis software were used for phase identification.

The porosity of the samples, P , was determined by weighing and using the compact NiTi density:

$$P = \left(1 - \frac{\rho_{por}}{\rho_{mon}} \right) \times 100\% \quad (1)$$

where ρ_{por} is the density of a porous sample or powder blank, and ρ_{mon} is the 6.45 g/cm³ density of compact NiTi. The average size of pores and walls of the porous NiTi skeleton was determined by the random secant method using the ImageJ software.^[13–15] The histograms of the distribution of pores and inter-pore bridges by size were constructed.

Results and discussion

Microscopy and structural analysis

The porous alloy structure characterization included the study of the geometric parameters of the porous metal matrix, the state of the surface of the pores, and the phase composition of the walls of the porous framework. General views of the cross-sections of porous samples obtained by the SHS method in open gas flow and closed reactors are shown in Fig. 2. The pore space of the samples obtained in open gas flow and closed reactors is homogeneous and does not have noticeable differences. The pore size and porosity of the porous framework were estimated from the optical images using quantitative metallography methods.^[14]

The size distribution of pores and walls of the porous SHS-NiTi frameworks obtained in closed and open gas flow reactors

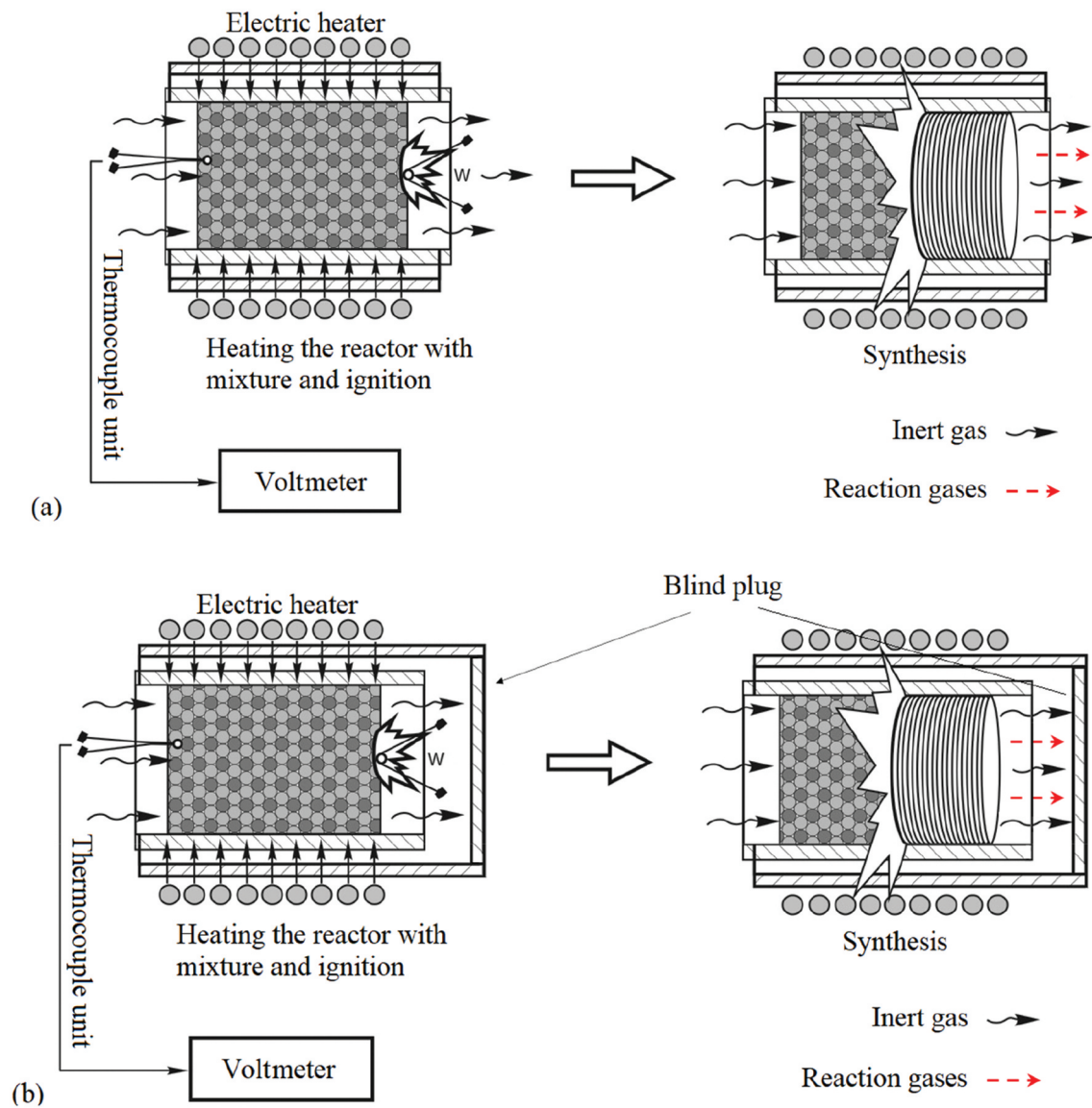


Figure 1. Schematics of the porous NiTi alloys production by the SHS method in (a) open gas flow and (b) closed reactors.

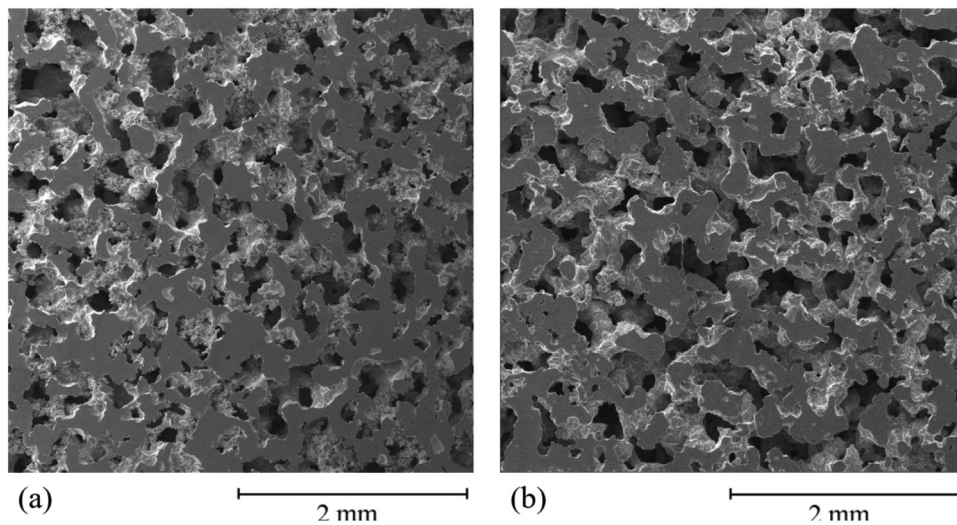


Figure 2. Macrostructure of the porous NiTi ingots obtained by the SHS method in (a) open gas flow and (b) closed reactors.

in an argon atmosphere has a unimodal logarithmically normal form, which is typical for fine porous materials. The histograms in Fig. 3 show that the maximum pore sizes and wall thickness of the sample obtained in a closed reactor is 800 μm in Fig. 3(a, b), while for the sample obtained in an open gas flow reactor, the maximum pore sizes and frame walls reach smaller values of 600 μm in Fig. 3(c, d).

The porosity of the samples obtained in the closed and open gas flow reactors was 66–64% and 62–60%, respectively, in Table 1. The closed reactor sample had an average pore size of $179 \pm 20 \mu\text{m}$ and an average wall thickness of $124 \pm 30 \mu\text{m}$, while the sample obtained in the open gas flow reactor had a smaller average pore size of $137 \pm 20 \mu\text{m}$ and $114 \pm 30 \mu\text{m}$ wall thickness. This effect is explained by the lower rate, heat and mass transfer of the reaction gases in a closed reactor and, as a result, the smaller contribution of the melt transferred from the reaction zone to the coalescence of all structural elements of the porous framework. When studying the phase composition of porous samples obtained in closed and open gas flow reactors by XRD, it was found that the alloys contain an austenitic TiNi phase with a B2 cubic structure, a martensitic TiNi phase with a B19' monoclinic structure,

along with Ti_2Ni and TiNi_3 phases in Fig. 4. It was not possible to determine the volume fraction of the detected phases due to the significant phase inhomogeneity of the alloys.

Cross-sections of porous SHS-NiTi samples synthesized in closed and open gas flow reactors were studied by SEM. Light gray dendrites formed of round 15–30 μm grains surrounded by a network of intergranular dark gray phases were found in the walls of the NiTi alloy synthesized in an open gas flow reactor. A dark-gray phase dispersed in the form of local accumulations of isolated 4–5 μm grains was found in the alloy synthesized in a closed reactor. Evenly distributed inclusions less than 2 μm in size were also observed. Microstructural studies of a porous alloy synthesized in an open gas flow reactor detected accumulations of larger grains localized in areas similar in shape and size to previously discovered dendrites in Fig. 5. Thus, the phase composition analysis of porous alloys obtained in the closed and open gas flow reactors revealed the distinctive features of the dark grey phase distribution, formed during peritectic crystallization. It has been established that, in addition to the regions of the NiTi solid solution, two-phase dendritic regions of peritectic crystallization are formed during synthesis in an open gas flow reactor,

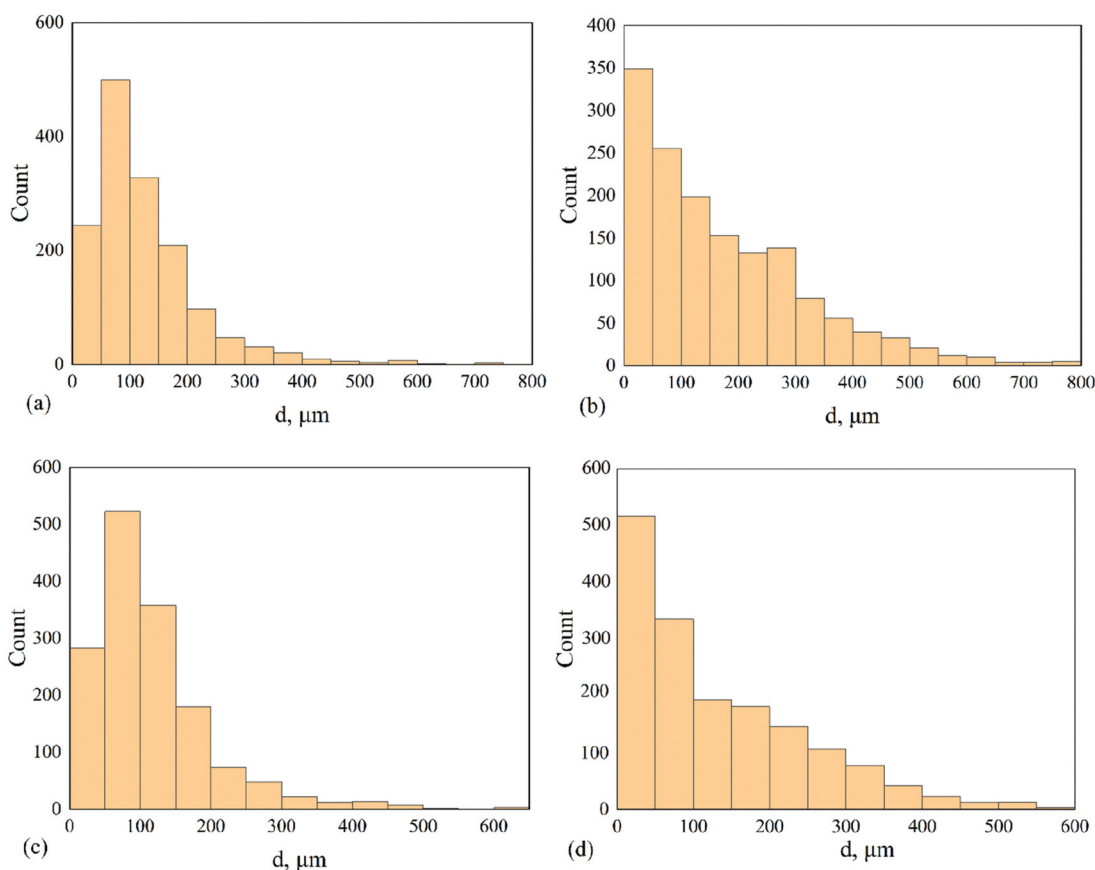


Figure 3. Histograms of the size distribution of (a, c) the frame walls and (b, d) pores in SHS-NiTi samples obtained in (a, b) closed and (c, d) open gas flow reactors.

Table 1. Dimensional parameters and porosity of the SHS-NiTi alloys obtained in closed and open gas flow reactors.

Alloy synthesized in:	$d_{\text{wall}}, \mu\text{m}$	$d_{\text{pore}}, \mu\text{m}$	P, %
Closed reactor	124-92	179-159	66-64
Open gas flow reactor	114-84	137-124	62-60

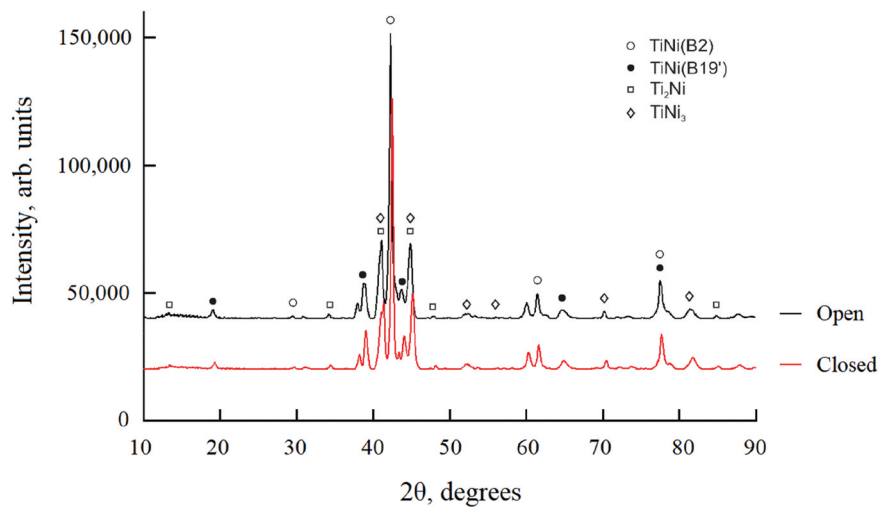


Figure 4. X-ray diffraction patterns of SHS products obtained in closed and open gas flow reactors.

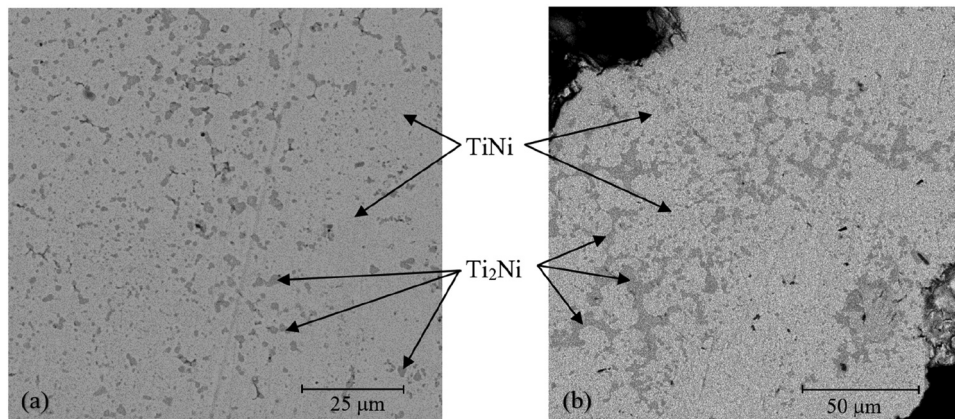


Figure 5. Cross-section SEM images of the sample walls obtained in (a) closed and (b) open gas flow reactors.

consisting of light gray rounded TiNi grains and an intergranular network of a dark gray Ti₂Ni phase. The samples synthesized in a closed reactor do not contain such structures. The observed variance in the phase composition of porous alloys is associated with different temperature distribution and amount of reaction heat in the closed and open gas flow reactors.

In a closed reactor, the inert Ar gas is mixed with the hot reaction gases and all the reaction heat stays in the reactor, annealing the crystallizing alloy. The areas of peritectic crystallization in the form of two-phase TiNi+Ti₂Ni dendrites, turn into the TiNi solid solution grains with the accumulation of secondary Ti₂Ni crystals as a result of annealing. The dispersion of the Ti₂Ni network phase into secondary grains makes its distribution in the matrix more uniform. In an open gas flow reactor, inert protective gas and hot reaction gases are removed from the reaction zone, carrying away excess heat and the crystallization of the alloy is faster than in a closed reactor.

Figure 6 shows the EDS maps of the Ti and Ni elements in the cross-section of porous SHS-NiTi samples obtained in closed and open gas flow reactors, which made it possible to determine the elemental composition of the peritectic crystallization regions.

Precipitates with a concentration composition close to the Ti₂Ni compound stoichiometry are found in Fig. 6(a, b). SEM micrograph in Fig. 6(a) of a porous SHS-NiTi sample obtained in a closed reactor shows a dispersed distribution of particles with Ti₂Ni stoichiometric composition. These particles are located in the grains of the TiNi matrix phase. It is seen from a porous SHS-NiTi sample obtained in an open flow reactor in Fig. 6(b) that the precipitated particles with the Ti₂Ni stoichiometric composition form grids. These grids are located between rounded 15–30 μm TiNi matrix grains. The presented data show that in a closed reactor, the distribution of the Ti₂Ni phase in the synthesis products is more uniform than in an open gas flow reactor.

The obtained data also indicate that, during synthesis in an open reactor, the reaction gases transfer heat from the reaction zone to the structuring zone, and then remove heat from the porous sample and the reactor to the environment, simultaneously heating the surface of the porous framework in the alloy structuring zone. In this process, the thermal effect of the reaction gases is sufficient to only maintain peritectic crystallization, during which an intergranular network phase is formed.

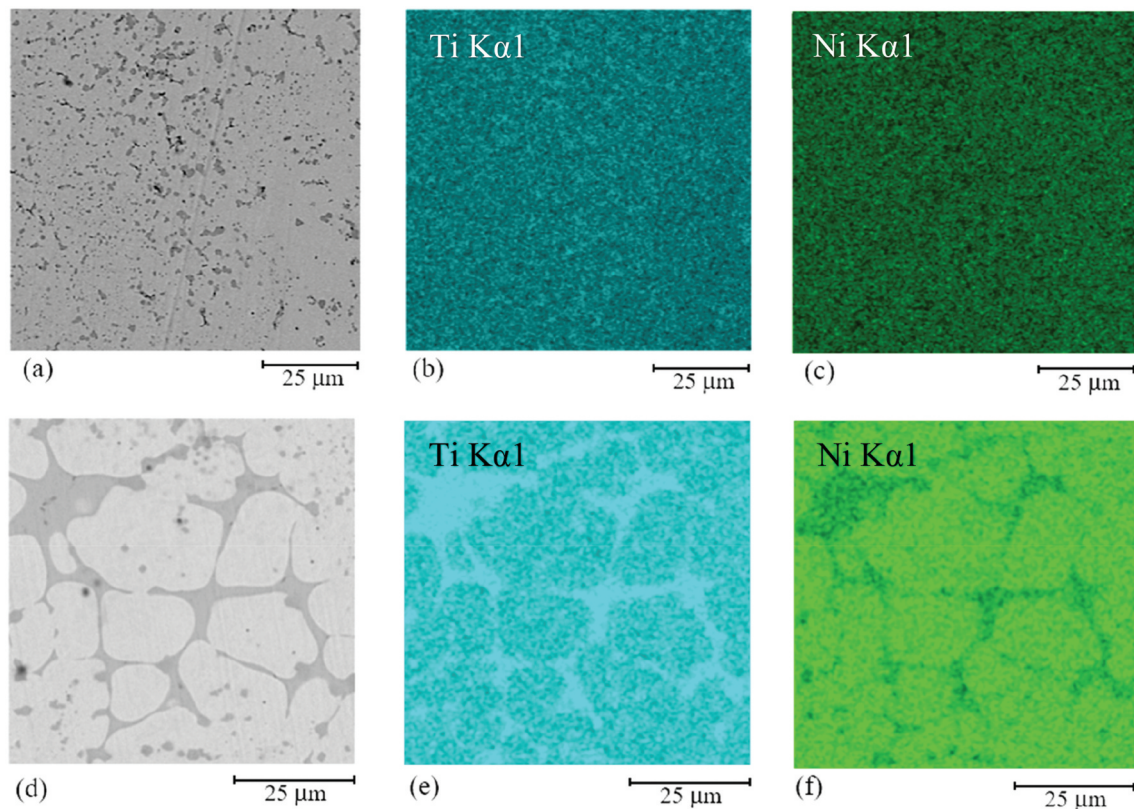


Figure 6. (a, d) SEM images and (b, c, e, f) EDS maps of Ti and Ni distribution in the peritectic crystallization zones of porous SHS-NiTi obtained in (a, b, c) closed and (d, e, f) open gas flow reactors.

Vacuum annealing and porous NiTi composition in an open reactor

To substantiate the possibility of dendrites recrystallization, the samples obtained in an open gas flow reactor were vacuum annealed at 1,200°C for 30 min, and the phase composition of the annealed samples was studied. The annealing temperature was chosen to achieve reliable dissolution of the Ti_2Ni phase in the TiNi matrix based on the previous experience of NiTi powders activated sintering. To obtain a strong bond between NiTi powder particles, it is necessary to heat the workpiece above the 984°C melting point of the Ti_2Ni phase, but below

the 1,310°C TiNi phase melting temperature. The appearance of the melt activates the recrystallization of the main TiNi phase. The holding time must be sufficient for the diffusion of the melt into the TiNi phase. The cross-sections of the samples were examined by optical microscopy after annealing. Recrystallized 20–250 μm wide zones were found near the porous sample surface with 5–40 μm isolated secondary phase crystals located along the TiNi grain boundaries in Fig. 7. No dendritic two-phase zones were found in the annealed samples, indicating that the chosen temperature and holding time were adequate to complete recrystallization. A solid solution

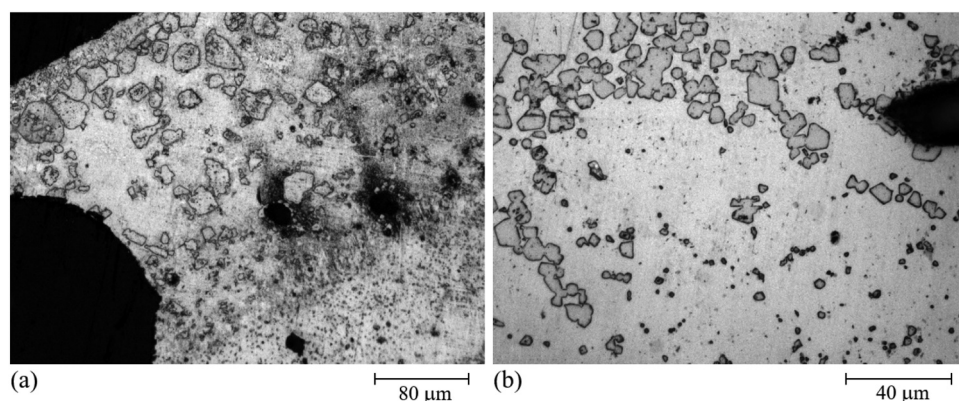


Figure 7. Optical micrographs of recrystallized specimens with secondary crystals: (a) recrystallized zone of peritectic crystallization and solid solution crystallization zone; (b) fragment of the zone border.

crystallization zone was found deeper below the surface and the recrystallization zone. It did not change its appearance as a result of annealing. No intergranular phase interlayers were found in this zone both before and after annealing. There are dispersed 1–2 μm inclusions inside the TiNi grains and larger 2–4 μm inclusions are present at the grain boundaries.

When heated above 984°C, the peritectic crystallization zone undergoes recrystallization and the Ti₂Ni+TiNi peritectic changes from a dendritic to crystalline form as a result. Isolated Ti₂Ni secondary phase crystals vary within the 5–40 μm size range depending on the primary dendrites' size, temperature, and recrystallization time.

Martensitic transformations in porous NiTi alloys

Figure 8 shows thermograms obtained by differential scanning calorimetry (DSC). An analysis of these thermograms made it possible to identify the temperature intervals and specific heat of direct and reverse martensitic transformations in Table 2.

A one-stage B2 \rightarrow B19' direct martensitic transformation was observed upon cooling samples obtained in closed and open gas flow reactors, while the reverse B19' \rightarrow B2 transformation was observed upon heating. The temperature ranges of forward and reverse MT do not depend on the reactor type. The temperature at the beginning of the direct martensitic transformation M_s for all samples is about 68.5°C, and the temperature at the end of the direct martensitic transformation M_f is about 57°C. The magnitude of the peak in the DSC curve characterizes the exothermic effect of the martensitic reaction and weakly depends on the reactor type. When samples of the

porous SHS-TiNi alloy are heated during the reverse B19' \rightarrow B2 martensitic transformation, heat is absorbed, and its amount also weakly depends on the reactor type. The temperatures of the onset A_s and end A_f of the reverse martensitic transformation were about 89°C and 107°C for both samples, respectively. These results are in agreement with the literature data for porous NiTi alloys.^[16–18]

The difference between the beginning and end temperatures of the reversible martensitic transformation did not exceed 0.5°C between the samples obtained in open gas flow and closed reactors. The effects of porous SHS-TiNi alloys synthesis temperature regimes can be considered insignificant compared with the vacuum annealing effects, which shift the martensitic transformation temperatures by 20–25°C.^[8] The difference between the specific heat values of the martensitic reaction did not exceed 0.4 J/g. This also confirmed the weak effect of the synthesis temperature regimes in the closed and open gas flow reactors on the course of martensitic transformations in the synthesized alloys.

Uniaxial compression of porous SHS-NiTi alloys

Deformation features of porous SHS-NiTi samples obtained in closed and open gas flow reactors were compared using uniaxial compression stress-strain curves in Fig. 9. The elastic region of both porous samples ends at 2–2.5% relative strain at point A corresponding to the elastic limit σ_{el} in compression curve 1 of the sample obtained in an open reactor and at point C in compression curve 2 of the sample obtained in a closed reactor. The accumulation of viscoelastic strain in both

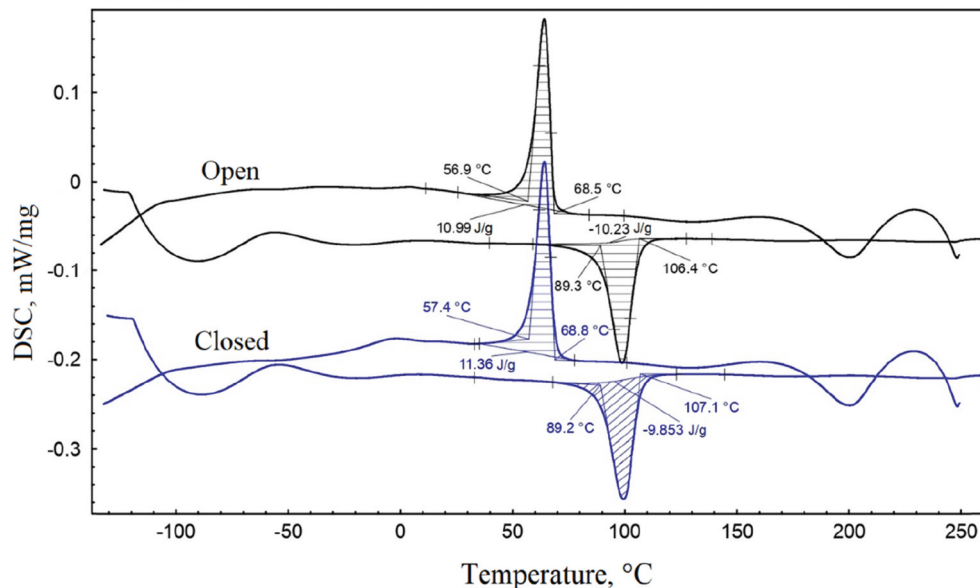


Figure 8. DSC thermograms of the SHS-NiTi samples obtained in closed and open gas flow reactors.

Table 2. Temperatures and heat capacity of direct and reverse martensitic transformations.

Reactor type	M_s , °C	M_f , °C	A_s , °C	A_f , °C	Heat capacity A→M, J/g	Heat capacity M→A, J/g
Open gas flow	68.5	56.9	89.3	106.4	10.99	-10.23
Closed	68.8	57.4	89.2	107.1	11.36	-9.85

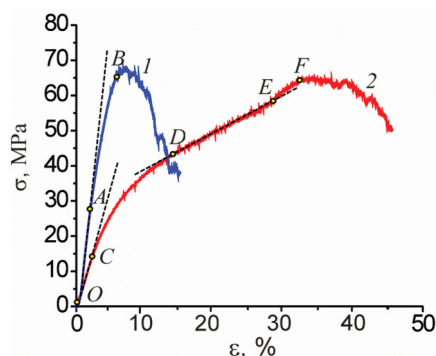


Figure 9. Compressive stress-strain curves of samples obtained in (1) open gas flow and (2) closed reactors. The dotted lines indicate areas of Hooke's linear deformation and linear hardening.

samples occurs in sections A – B and C – F, respectively (Fig. 9, curves 1 and 2). Compression in both samples ends with stepwise destruction of the porous framework. In deformation curve 1, viscoelastic strain slightly deviates from elastic strain and ends at 5%, corresponding to the total accumulated strain. Curve 2 shows an extended section of 14–28% of linear hardening D – E due to plastic deformation. It contributes approximately 15% to the total accumulated strain, which reaches 34%.

The effective stiffness of samples obtained in an open gas flow reactor is significantly higher than the samples obtained in a closed reactor. However, the accumulated plastic deformation of the samples synthesized in a closed reactor is much higher than in an open gas flow reactor in Table 3.

In the compression curves of samples obtained in open gas flow and closed reactors, no yield points were found, which are usually associated with plastic deformation of the walls of the porous framework in ductile alloys. The results of this study showed that the SHS thermal regime significantly affects the viscoelastic properties of the porous NiTi alloy. The effective stiffness of the samples obtained in an open gas flow reactor is significantly higher than the samples obtained in a closed reactor. However, the accumulated plastic deformation of the samples synthesized in a closed reactor is much higher than in an open gas flow reactor. During synthesis in an open gas flow and closed reactors, heat transfer from the reaction zone to the structuring zone is carried out by filtering the reaction gases through the synthesized primary porous framework, modifying its phase composition.^[19] As a result, a peritectic crystallization zone with a fragile network of the Ti₂Ni intergranular phase is formed. The thermal effect of the evolved reaction gases is the cause of both peritectic crystallization zone formation and its recrystallization. However, due to the longer and more intense thermal effect of the exothermic reaction heat, the two-phase TiNi+Ti₂Ni zone successfully recrystallizes in a closed reactor. In this case, the primary network of the Ti₂Ni intergranular phase is dispersed and separate secondary Ti₂Ni

phase crystals are formed. Thus, the different nature of the Ti₂Ni phase distribution affects the mechanical properties of the porous NiTi alloy. While remaining brittle, secondary phase crystals have little effect on the plastic properties of NiTi grains. Therefore, samples obtained in a closed reactor have a lower effective stiffness of 0.67 GPa versus 1.8 GPa for samples synthesized in an open gas flow reactor. The uniform distribution of secondary crystals from the Ti₂Ni phase during alloy synthesis in an open gas flow reactor does not interfere with the high plasticity of the TiNi-based matrix phase under uniaxial compression up to 34% and does not increase the brittleness of the porous NiTi alloy.

Conclusions

Samples of a porous NiTi alloy were obtained by the SHS method using the layer-by-layer combustion mode in an open gas flow and closed reactors. The study of porous samples by XRD and DSC methods showed that the main phase of the porous alloy is the TiNi intermetallic compound, which experiences a reversible martensitic transition above room temperature during thermal cycling. EDS mapping and SEM studies have shown that the alloy contains two-phase zones of peritectic crystallization (TiNi+Ti₂Ni), which when synthesized in an open reactor have a dendritic form, and when synthesized in a closed reactor have a crystalline form. Compression tests of porous SHS-TiNi samples were carried out, which showed that samples obtained in a closed reactor due to an additional 25% plastic deformation accumulate 5 times more deformation than samples from an open gas flow reactor. Rigid dendrites of the Ti₂Ni phase prevent plastic deformation of the matrix, increase the effective rigidity of the samples, and reduce the accumulated plastic deformation of porous samples. Accumulations of Ti₂Ni crystals do not limit the plastic deformation of TiNi grains and do not increase the effective rigidity of porous samples. The samples obtained in an open gas flow reactor were additionally annealed in a vacuum at 1,210°C for 30 minutes. By comparing the samples before and after annealing using optical microscopy, it was found that, upon annealing in a vacuum, the two-phase dendrites of the peritectic zone undergo recrystallization and turn into a crystalline two-phase zone. The obtained results allow stating that SHS in a closed reactor makes it possible to obtain a more ductile porous NiTi alloy with a more perfect phase composition due to the additional thermal contribution of the reaction gases.

Acknowledgments

This research was supported by the Mega grant from the Government of the Russian Federation No. 220 of 09 April 2010 (Agreement No. 075-15-2021-612 of 04 June 2021). The characterization was carried out using the equipment of the Tomsk Regional Core Shared Research Facilities Center of the National Research Tomsk State University, supported by the grant of the Ministry of Science and Higher Education of the Russian Federation 075-15-2021-693 (No. 13.RFC.21.0012).

Disclosure statement

No potential conflict of interest was reported by the author(s).








Table 3. Mechanical properties of porous SHS-NiTi samples obtained in closed and open gas flow reactors.

Reactor type	E, GPa	σ_{el} , MPa	σ_U , MPa	ϵ_f , %
Open gas flow	1.8±0.1	28±3	67±3	7±0.5
Closed	0.67±0.1	14±3	65±3	34±0.5

Funding

The work was supported by the Government of the Russian Federation [075-15-2021-612]; Ministry of Science and Higher Education of the Russian Federation [075-15-2021-693].

ORCID

Ekaterina S. Marchenko  <http://orcid.org/0000-0003-4615-5270>
 Yuri F. Yasenchuk  <http://orcid.org/0000-0003-1364-6559>
 Oibek Mamazakirov  <http://orcid.org/0000-0002-7457-0714>
 Anatoly A. Klopotov  <http://orcid.org/0000-0002-3690-0436>
 Gulsharat A. Baigonakova  <http://orcid.org/0000-0001-9853-2766>
 Alex A. Volinsky  <http://orcid.org/0000-0002-8520-6248>
 Sergey V. Gunter  <http://orcid.org/0000-0001-6963-2047>

References

- [1] Gunter, V.; Yasenchuk, Y.; Gunther, S.; Marchenko, E.; Yuzhakov, M. Biocompatibility of Porous SHS-TiNi. *Mater. Sci. Forum.* 2019, 970, 320–327. <https://www.scientific.net/MSF.970.320>.
- [2] Yasenchuk, Y.; Marchenko, E.; Gunther, V.; Radkevich, A.; Kokorev, O.; Gunther, S.; Baigonakova, G.; Hodorenko, V.; Chekalkin, T.; Kang, J. H., et al. Biocompatibility and Clinical Application of Porous TiNi Alloys Made by Self-Propagating High-Temperature Synthesis (SHS). *Mater.* 2019, 12(15), 2405.
- [3] Patel, S. K.; Roshan, R. 6 - NiTi superalloys. In *Micro and Nano Technologies*; Thomas, S., Behera, A., and Nguyen, T. A., Eds.; Amsterdam, Netherlands: Nickel-Titanium Smart Hybrid Materials, Elsevier, 2022; pp. 105–122.
- [4] Jonathan, C. Y.; Chu, C. L.; Wang, S. D. Porous TiNi Shape Memory Alloy with High Strength Fabricated by Self-Propagating High-Temperature Synthesis. *Mater. Lett.* 2004, 58(11), 1683–1686. DOI: 10.1016/j.matlet.2003.10.045.
- [5] Lis, J. Self-Propagating High-Temperature Synthesis. In *Encyclopedia of Materials: Technical Ceramics and Glasses*; Pomeroy, M., Ed.; Amsterdam, Netherlands: Elsevier, 2021; pp. 40–58.
- [6] Whitney, M.; Corbin, S. F.; Gorbet, R. B. Investigation of the Influence of Ni Powder Size on Microstructural Evolution and the Thermal Explosion Combustion Synthesis of NiTi. *Intermetallics.* 2009, 17(11), 894–906. DOI: 10.1016/j.intermet.2009.03.018.
- [7] Bertolino, N.; Monagheddu, M.; Tacca, A.; Giuliani, P.; Zanotti, C.; Anselmi Tamburini, U. Ignition Mechanism in Combustion Synthesis of Ti–Al and Ti–Ni Systems. *Intermetallics.* 2003, 11(1), 41–49. DOI: 10.1016/S0966-9795(02)00128-0.
- [8] Khodorenko, V. N.; Guenther, V. E.; Soldatova, M. I. Influence of Heat Treatment on Shape Memory Effect in Porous Titanium Nickel Synthesized by the SHS Process. *Russ. Phys. J.* 2011, 53(10), 1024–1034. DOI: 10.1007/s11182-011-9526-2.
- [9] Khodorenko, V. N.; Gyunter, V. E. Investigations of the Structure of Porous Titanium Nickelide After Thermal Treatment. *Russ. Phys. J.* 2009, 51(10), 1090–1096. DOI: 10.1007/s11182-009-9146-2.
- [10] Tang, W.; Shen, Q.; Yao, X.; Li, W.; Jiang, J.; Ba, Z.; Li, Y.; Shi, X. Effect of Grain Size on the Microstructure and Mechanical Anisotropy of Stress-Induced Martensitic NiTi Alloys. *Mater. Sci. Eng. A.* 2022, 849, 849, 143497. DOI: 10.1016/j.msea.2022.143497.
- [11] Akopyan, T.; Padalko, A.; Belov, N.; Shurkin, P. Effect of a High Temperature and Hydrostatic Pressure on the Structure and the Properties of a High-Strength Cast AM5 (The 201.2 Alloy Type) Aluminum Alloy. *Russ. Metall. (Met.).* 2016, 2016(7), 657–662. DOI: 10.1134/S0036029516070028.
- [12] Saadati, A.; Aghajani, H. Fabrication of Porous NiTi Biomedical Alloy by SHS Method. *J. Mater. Sci.: Mater. Med.* 2019, 30(8), 92. DOI: 10.1007/s10856-019-6296-9.
- [13] Saltykov, S. A. *Stereometric Metallography*; Moscow: Metallurgy, 1976.
- [14] Carlos, A.; Mendiola-Santibañez; Paredes-Orta, F.; Jorge, D.; Terol-Villalobos, I. R. Method for Grain Size Determination in Carbon Steels Based on the Ultimate Opening. *Measurement.* 2019, 133, 193–207. DOI: 10.1016/j.measurement.2018.09.068.
- [15] Lawley, A.; Murphy, T. F. Metallography of Powder Metallurgy Materials. *Mater. Charact.* 2003, 51(5), 315–327. DOI: 10.1016/j.matchar.2004.01.006.
- [16] Aihara, H.; Zider, J.; Fanton, G.; Duerig, T. Combustion Synthesis Porous NiTiInol for Biomedical Applications. *Int. J. Biomater.* 2019, 2019(2), 1–11. DOI: 10.1155/2019/4307461.
- [17] Otsuka, K.; Ren, X. Physical Metallurgy of Ti–ni-Based Shape Memory Alloys. *Prog. Mater. Sci.* 2005, 50(5), 511–678. DOI: 10.1016/j.pmatsci.2004.10.001.
- [18] Bolokanga, A. S.; Mathabathe, M. N.; Chikosha, S.; Motaung, D. E. Investigating the Heat Resistant Properties of the TiNi Shape Memory Alloy on the B19'→B2 Phase Transformation Using the Alloy Powder. *Surf. Interfaces.* 2020, 20, 100608. DOI: 10.1016/j.surfin.2020.100608.
- [19] Yasenchuk, Y.; Gunther, V.; Marchenko, E.; Chekalkin, T.; Baigonakova, G.; Hodorenko, V.; Gunther, S.; Kang, J. -H.; Weiss, S.; Obrosof, A. Formation of Mineral Phases in Self-Propagating High-Temperature Synthesis (SHS) of Porous TiNi Alloy. *Mater. Res. Express.* 2019, 6(5), 056522. DOI: 10.1088/2053-1591/ab01a1.